Journal of Solid Mechanics Vol. 10, No. 4 (2018) pp. 688-701

Effect of Follower Force on Vibration Frequency of Magneto-Strictive-Faced Sandwich Plate with CNTR Composite Core

M.R. Ghorbanpour Arani [1,*], Z. Khoddami Maraghi [2]

[1]*Electrical Engineering Department, Amirkabir University of Technology, Tehran, Iran*
[2]*Faculty of Mechanical Engineering, University of Kashan, Kashan, Iran*

Received 30 June 2018; accepted 31 August 2018

ABSTRACT

This study deals with the vibration response of sandwich plate with nano-composite core and smart magneto-strictive face sheets. Composite core is reinforced by carbon nanotubes (CNTs) and its effective elastic properties are obtained by the rule of Mixture. Terfenol-D films are used as the face sheets of sandwich due to magneto-mechanical coupling in magneto-strictive material (MsM). In order to investigate the magnetization effect on the vibration characteristics of sandwich plate, a feedback control system is utilized. Also the sandwich plate undergoes the follower forces in opposite direction of x. Based on energy method, equations of motions are derived using Reddy's third order shear deformation theory, and Hamilton's principle and solved by differential quadrature method (DQM). A detailed numerical study is carried out based on third-order shear deformation theory to indicate the significant effect of follower forces, volume fraction of CNTs, temperature change, core-to-face sheet thickness ratio and controller effect of velocity feedback gain on dimensionless frequency of sandwich plate. These finding can be used to automotive industry, aerospace and building industries.

Keywords: Sandwich plate; Follower force; Feedback control system; Nano-composite; Magneto-strictive sheets.

1 INTRODUCTION

COMPOSITE materials are consisted of two or more materials which together produce desirable properties that cannot be achieved with any of the constituents alone. Almost, fibers with high strength and high modulus are used in a matrix material of composite [1]. Different types of fibers and matrix are utilized in composites to product a material with high quality. Composites are used in many industries including aerospace, shipping industry, building bridges etc. Composite materials and sandwich structures have long been of interest to researchers but in recent decades, smart materials have created a breakthrough in the investigation. Panda and Ray [2] studied nonlinear dynamic analysis of functionally graded (FG) laminated composite plates integrated with a patch. Piezoelectric fiber reinforced composite (PFRC) material was used for constraining layer of the active constrained layer damping (ACLD) treatment. In this regard, fiber-reinforced composite material was considered for each layer of the substrate FG laminated composite plate. Based on the first-order shear deformation (FSDT) theory, a finite

*Corresponding author. Tel.: +98 3155912450; Fax: +98 3155912424.
E-mail address: mrezagh6193@gmail.com (M.R.Ghorbanpour Arani).

element model was developed and the effect of piezoelectric fiber on the damping characteristics of the overall FG plates was investigated. Wang and Shen [3] investigated the large amplitude vibration a sandwich plate with carbon nanotube-reinforced composite (CNTRC) face sheets resting on an elastic foundation in thermal environments. They used micromechanical model to estimate the material properties of CNTRC face sheets. Their results showed the effects of nanotube volume fraction, core-to-face sheet thickness ratio, temperature change, foundation stiffness and in-plane boundary conditions on the nonlinear vibration characteristics of sandwich plates. Free vibration analysis of FG nano-composite plates reinforced by single walled carbon nanotubes (SWCNTs) was presented by Lei et al. [4] using the element-free kp-Ritz method. The composite was assumed to be graded through the thickness direction according to several linear distributions of the volume fraction of CNTs. They also presented in several examples the effects of CNT volume fraction, width-to-thickness ratio, aspect ratio and temperature change on natural frequencies and mode shapes of FG-CNTRC plates. Bending and free flexural vibration behavior of sandwich plates with CNT reinforced face sheets were developed by Natarajan et al. [5] based on higher-order structural theory. They considered the in-plane and rotary inertia terms in the formulation. In this work, the governing equations were solved for sandwich plate with homogeneous core and CNT reinforced face sheets. They examined the influence of volume fraction of the CNT, core-to-face sheet thickness and thickness ratio on the global/local response of different sandwich plates. Vibration of laminated plates resting on Pasternak foundation was investigated by Malekzadeh et al. [6] considering the effect of non-ideal boundary conditions and initial stresses due to in-plane loads. They used the Lindstedt–Poincare perturbation technique to solve the problem and obtained the frequencies and mode shapes of the plate. They also compared their result with finite element simulation, using ANSYS software. Also they showed the effect of various parameters like stiffness of foundation, boundary conditions and in-plane stresses on the vibration of the plate. Lee et al. [7] studied the transient response of laminated composite plates with embedded smart material layers using a unified plate theory that includes the classical, first-order, and third-order plate theories. Terfenol-D layers were used to control the vibration suppression. Their findings showed the effect of material properties, smart layer position, and smart layer thickness on the vibration suppression of plate. Hong [8] studied the transient response of thermal stresses and center displacement in laminated magneto-strictive plates under thermal vibration. He also used the velocity feedback control to vibration suppression in a three-layer laminated magneto-strictive plate with four simply supported edges. His results showed an efficient method to compute the results including shear deformation effect with a few grid points. Dynamic stability analysis of an isotropic, orthotropic and a symmetrically laminated composite plate under a pure follower force was performed by Kim and Kim [9]. Kirchhoff-Love and Mindlin plate theory were utilized to theoretical analysis and its results were compared with finite element method. Jayaraman and Struthers [10] analyzed the divergence and flutter instabilities of a rectangular, orthotropic plate subject to follower forces. They discussed the effects of the tangential follower parameter, aspect ratio, boundary condition, and the magnitude of the critical load on the stability of plate. Guo et al. [11] studied the dynamic characteristics and stability of rectangular plate subjected to uniformly distributed tangential follower force. They presented the differential equation of motion considering thermo-elastic coupling for rectangular plate under tangential follower force. They calculated the dimensionless complex frequencies of the moving rectangular plate for different boundary conditions. Dynamic behavior of a non-uniform column reinforced by single-walled CNTs resting on an elastic foundation and subjected to follower force was investigated by Pourasghar and Kamarian [12]. In this work, the CNTRC columns have smooth variation of CNT fraction in the thickness direction and the material properties were estimated by the extended rule of mixture.

Free vibration of nano-composite sandwich plate made of two smart magneto-strictive face sheets is a new topic that cannot be found in literature. MsM due to reciprocal nature is one of the most affordable options in control systems. Magneto-mechanical coupling in these materials feels a connection between stress and magnetization that can be used in stability of systems. In this research core-to-face sheet thickness ratio is considered large and magneto-strictive sheets acts in a feedback control system. In this work, effect of follower forces are studied when the forces applied in opposite direction of x axis. The results of this study investigate the effect of important parameters on vibrational behaviour of sandwich plate that can be useful in many industries.

2 STRUCTURAL DEFINITION

Fig. 1 shows a schematic diagram of a sandwich plate with geometrical parameters of length *a*, width *b* and thickness $2h_m + h_c$.

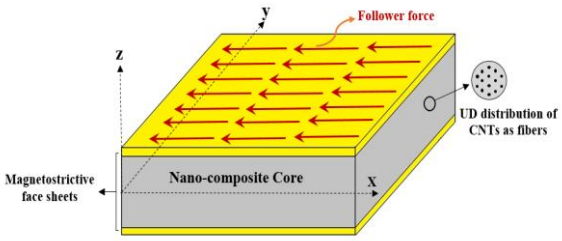

Fig.1
A schematic figure.

As shown in Fig. 1 the structure that studied in this paper is composed of three layers:

- ❖ Central core reinforced by CNT,
- ❖ Two face sheets made of MsM.

The strain-displacement relations are separately written for each of the layers, then forces and moments are obtained. Finally the total energy equation which includes the energy of CNTRC core and magneto-strictive face sheet are obtained using the Hamilton's principle considering follower forces.

3 CONSTITUTIVE EQUATIONS

Stress-strain relation for isotropic material shows in Eq. (1) [1]:

$$\begin{bmatrix}\sigma_{xx}\\ \sigma_{yy}\\ \sigma_{xy}\\ \sigma_{xz}\\ \sigma_{yz}\end{bmatrix}=\begin{bmatrix}\bar{Q}_{11} & \bar{Q}_{12} & 0 & 0 & 0\\ \bar{Q}_{21} & \bar{Q}_{22} & 0 & 0 & 0\\ 0 & 0 & \bar{Q}_{44} & 0 & 0\\ 0 & 0 & 0 & \bar{Q}_{55} & 0\\ 0 & 0 & 0 & 0 & \bar{Q}_{66}\end{bmatrix}\begin{bmatrix}\varepsilon_{xx}\\ \varepsilon_{yy}\\ \varepsilon_{xy}\\ \varepsilon_{xz}\\ \varepsilon_{yz}\end{bmatrix} \tag{1}$$

where σ_{ij} and Q_{ij} are normal and shear stresses and the terms of engineering constants:

$$\bar{Q}_{11}=\bar{Q}_{22}=\frac{E}{(1-\upsilon^2)},\quad \bar{Q}_{12}=\bar{Q}_{13}=\frac{E\upsilon}{(1-\upsilon^2)},\quad \bar{Q}_{44}=\bar{Q}_{55}=\bar{Q}_{66}=\frac{E}{(1+\upsilon)} \tag{2}$$

In which E and υ are Young modulus and Poisson's ratio respectively. Eqs. (1) and (2) are valid for CNTRC core and magneto-strictive face sheets ($\bar{C}_{ij}$ instead $\bar{Q}_{ij}$). Sections (3.1) and (3.2) are presented the elastic properties of central core that reinforced by CNTs and magneto-strictive face sheet.

3.1 Mechanical properties of CNTRC core

Consider a CNTRC plate with thickness h_c and dimensions $(a\times b)$ .This CNTRC plate is made of different isotropic material that called fibers (SWCNT) and matrix (*PmPV*). The fibers reinforcement is uniformly distributed in length of plate. According to the extended rule of mixture, the material properties of CNTRC plates can be expressed as [4]:

$$\begin{aligned}&E_{11}=\eta_1 V_{CNT}E_{11}^{CNT}+V_m E^m,\\ &\frac{\eta_2}{E_{22}}=\frac{V_{CNT}}{E_{22}^{CNT}}+\frac{V_m}{E^m},\\ &\frac{\eta_3}{G_{12}}=\frac{V_{CNT}}{G_{12}^{CNT}}+\frac{V_m}{G^m}\end{aligned} \tag{3}$$

where E_{11}^{CNT} , E_{22}^{CNT} ,G_{12}^{CNT} , E_m and G_m are the Young's moduli and shear modulus of CNT and isotropic matrix. To account load transfer between the fibers and matrix such as the surface effect, strain gradient effect, and intermolecular coupled effect on the equivalent material properties of CNTRCs, CNT efficiency parameters η_j (j = 1,2, 3) introduced by Shen [13] in Eq. (3) [4]. V_{CNT} and V_m are the volume fractions of CNT and matrix. Poisson's ratio is also introduced as follows [4]:

$$\upsilon_{12} = V_{CNT}\upsilon_{12}^{CNT} + V_m\upsilon^m, \tag{4}$$

where υ_{12}^{CNT} and υ_m are Poisson's ratios of fibers and matrix, respectively.

Lei et al. stated in Ref. [4] that the effective thickness of fibers plays an important role to estimate the material properties of CNTs. Han and Elliott [14] obtained a new value for SWCNTs (10,10) with $h = 0.34\,nm$, presented in Table 1:

Table 1
Material properties of SWCNTs (10,10) with $h = 0.34\,nm$.[4]

Han and Elliott [14]	E_{11}^{CNT}	E_{22}^{CNT}	G_{12}^{CNT}
SWCNTs (10,10)	600 *GPa*	10 *GPa*	17.2 *GPa*

Typical values of effective material properties of (10,10) SWCNTs with $h = 0.067\,nm$ for different temperature are listed in Table 2 [3,4,5]:

Table 2
Material properties of SWCNTs (10,10) with $h = 0.067\,nm$.[3,4,5]

SWCNT (10,10) ($L = 9.26\,nm$, $R = 0.68\,nm$, $h = 0.067\,nm$, $\upsilon_{12}^{CNT} = 0.175$)			
Temperature(K)	E_{11}^{CNT} (TPa)	E_{22}^{CNT} (TPa)	G_{12}^{CNT} (TPa)
300	5.6466	7.0800	1.9445
500	5.5308	6.9348	1.9643
700	5.4744	6.8641	1.9644

Comparing the results of extended rule of mixture and molecular dynamic (MD) simulations, the CNT efficiency parameter is estimated. Such as documented results that have been reported in Table 3 [13,14].

Table 3
CNT efficiency parameter for $V_{CNT} = 0.11, 0.14, 0.17$. [13, 14]

V_{CNT}	Rule of Mixture	
	η_1	η_2
$V_{CNT} = 0.11$	0.149	0.934
$V_{CNT} = 0.14$	0.150	0.941
$V_{CNT} = 0.17$	0.149	1.381

3.2 Magneto-striction effect

To consider the effect of magnetic field on MsM, the magneto-mechanical coupling for isotropic MsM can be observed in the following matrix [8]:

$$\begin{bmatrix} \sigma^{m}_{xx} \\ \sigma^{m}_{yy} \\ \sigma^{m}_{xy} \end{bmatrix} = -\begin{bmatrix} 0 & 0 & e_{31} \\ 0 & 0 & e_{32} \\ 0 & 0 & e_{34} \end{bmatrix} \begin{bmatrix} 0 \\ 0 \\ H_z \end{bmatrix}. \tag{5}$$

Index *m* refers to magnetic stress that summarized by Eq. (1) ($\bar{C}_{ij}$ instead $\bar{Q}_{ij}$). H_z and e_{ij} are the magnetic field intensity and the magneto-strictive coupling modules that can be expressed as follows [15,16, 8]:

$$H_z = K_c I(x,y,t) = K_c C(t) \frac{\partial w_0(x,y,t)}{\partial t} \tag{6}$$

where $K_c, I(t)$ and $C(t)$ are the coil constant, coil current and the control gain in which $K_c C(t)$ is introduced as velocity feedback gain.

Also e_{ij} are determined as follow [15]:

$$\begin{aligned} e_{31} &= \tilde{e}_{31}\cos^2\theta + \tilde{e}_{32}\sin^2\theta, \\ e_{32} &= \tilde{e}_{31}\sin^2\theta + \tilde{e}_{32}\cos^2\theta, \\ e_{34} &= (\tilde{e}_{31} - e_{32})\sin\theta\sin\theta \end{aligned} \tag{7}$$

where θ represents the direction of magnetic anisotropy.

4 THIRD ORDER SHEAR DEFORMATION THEORY (TSDT)

TSDT extends the FSDT by assuming that:

Shear strain and consequently shear stress are not constant through the plate thickness where for a moderately thick plate, TSDT leads to better results.

- The strain equations do not need a shear correction factor.
- The displacement field accommodates a quadratic variation of the transverse shear through the thickness and the vanishing of transverse shear stresses on the top and bottom surfaces of the plate [17, 18].

The displacement field of TSDT for plates is given by [18]:

$$\begin{aligned} \tilde{U}(x,y,z,t) &= u_0(x,y,t) + z\,\theta_1(x,y,t) - \frac{4}{3}\frac{z^3}{h^2}\left(\theta_1(x,y,t) + \frac{\partial}{\partial x} w_0(x,y,t)\right), \\ \tilde{V}(x,y,z,t) &= v_0(x,y,t) + z\,\theta_2(x,y,t) - \frac{4}{3}\frac{z^3}{h^2}\left(\theta_2(x,y,t) + \frac{\partial}{\partial y} w_0(x,y,t)\right), \\ \tilde{W}(x,y,z,t) &= w_0(x,y,t) \end{aligned} \tag{8}$$

where $u_0(x,y,t)$, $v_0(x,y,t)$, $w_0(x,y,t)$ are displacement function along (x,y,z) direction and $\theta_1(x,y,t)$, $\theta_2(x,y,t)$ are rotations about *x* and *y* axis and *t* is time. Sandwich plate is considered as a monolithic stricture where the displacement of each layers are assumed to be same according to Eq. (7).

The linear strain field for TSDT obtained by using Hooke's law, can be given as:

$$
\begin{aligned}
\varepsilon_{xx} &= \frac{\partial}{\partial x}u_0(x,y,t)+z\frac{\partial}{\partial x}\theta_1(x,y,t)-\frac{4}{3}\frac{z^3}{h^2}\left(\frac{\partial}{\partial x}\theta_1(x,y,t)+\frac{\partial^2}{\partial x^2}w_0(x,y,t)\right),\\
\varepsilon_{yy} &= \frac{\partial}{\partial y}v_0(x,y,t)+z\frac{\partial}{\partial y}\theta_2(x,y,t)-\frac{4}{3}\frac{z^3}{h^2}\left(\frac{\partial}{\partial y}\theta_2(x,y,t)+\frac{\partial^2}{\partial y^2}w_0(x,y,t)\right),\\
\varepsilon_{zz} &= 0\\
\varepsilon_{xy} &= \frac{1}{2}\frac{\partial}{\partial x}v_0(x,y,t)+\frac{1}{2}z\frac{\partial}{\partial x}\theta_2(x,y,t)-\frac{2}{3}\frac{z^3}{h^2}\left(\frac{\partial}{\partial x}\theta_2(x,y,t)+\frac{\partial^2}{\partial y\,\partial x}w_0(x,y,t)\right),\\
&\quad+\frac{1}{2}\frac{\partial}{\partial y}u_0(x,y,t)+\frac{1}{2}z\frac{\partial}{\partial y}\theta_1(x,y,t)-\frac{2}{3}\frac{z^3}{h^2}\left(\frac{\partial}{\partial y}\theta_1(x,y,t)+\frac{\partial^2}{\partial y\,\partial x}w_0(x,y,t)\right),\\
\varepsilon_{xz} &= \frac{1}{2}\frac{\partial}{\partial x}w_0(x,y,t)+\frac{1}{2}\theta_1(x,y,t)-2\frac{z^2}{h^2}\left(\theta_1(x,y,t)+\frac{\partial}{\partial x}w_0(x,y,t)\right),\\
\varepsilon_{yz} &= \frac{1}{2}\frac{\partial}{\partial y}w_0(x,y,t)+\frac{1}{2}\theta_2(x,y,t)-2\frac{z^2}{h^2}\left(\theta_2(x,y,t)+\frac{\partial}{\partial y}w_0(x,y,t)\right)
\end{aligned}
\tag{9}
$$

5 ENERGY METHOD IN SANDWICH PLATE

The energy method is used to obtain the governing equation, strain energy of the rectangular sandwich plate is calculated as [19]:

$$
\begin{aligned}
U &= \frac{1}{2}\int_V\left(\sigma_{xx}\varepsilon_{xx}+\sigma_{yy}\varepsilon_{yy}+\tau_{xy}\gamma_{xy}+\tau_{xz}\gamma_{xz}+\tau_{yz}\gamma_{yz}\right)dV,\\
U_{sandwich} &= U_{Core}+U_{Face\,sheets} = \frac{1}{2}\int_{-\frac{h_c}{2}}^{\frac{h_c}{2}}\int_0^b\int_0^a\left(\sigma_{ij}\varepsilon_{ij}+\tau_{ij}\gamma_{ij}\right)_{Core}dx\,dy\,dz,\\
&+\frac{1}{2}\int_{-h_m}^{-\frac{h_c}{2}}\int_0^b\int_0^a\left(\sigma_{ij}\varepsilon_{ij}+\tau_{ij}\gamma_{ij}\right)_{Sheet}dx\,dy\,dz+\frac{1}{2}\int_{\frac{h_c}{2}}^{\frac{h_c}{2}+h_m}\int_0^b\int_0^a\left(\sigma_{ij}\varepsilon_{ij}+\tau_{ij}\gamma_{ij}\right)_{Sheet}dx\,dy\,dz
\end{aligned}
\tag{10}
$$

Substituting Eqs. (1,5,9) into Eq. (10), the strain energy of sandwich plate can be obtained.
The kinetic energy of sandwich plate can be stated as [20]:

$$
K_{Sandwich} = K_{Core}+K_{Face\,sheets} = \frac{1}{2}(\rho_c h_c+2\rho_m h_m)\left(\int_0^b\int_0^a\left[\left(\frac{\partial\tilde{U}}{\partial t}\right)^2+\left(\frac{\partial\tilde{V}}{\partial t}\right)^2+\left(\frac{\partial\tilde{W}}{\partial t}\right)^2\right]dx\,dy\right) \tag{11}
$$

Substituting Eq. (8) into Eq. (11), the kinetic energy are obtained.

6 FOLLOWER FORCE

In one of the divisions, external forces are divided into two groups [9]:

- Conservative force such as in-plane forces which maintains a direction when the deformation occurs.

- ❖ Non-conservative force such as follower force which changes the direction according to the deformation such as hydraulic pressure, gas flow or magnetic field interactive forces acting on micro-structures.

Flutter and divergence instability are discussed when the follower force acts on the structure. A follower force follows the geometry as it deflects. It is applicable to geometrically problems where deflection is relatively large. In the other hand, the load direction is continuously updated based on the deflected geometry [11]. Eq. (12) presents the term that included follower force or the variation of done work by follower force:

$$F_{Follower\,force} = q(a-x)\frac{\partial^2 W}{\partial x^2} \tag{12}$$

In this work, follower force is applied on MsP as an external. Therefore, the external work due to orthotropic elastic foundation is calculated as:

$$\Sigma = \frac{1}{2}\int_0^b\int_0^a F_{Follower\,force} W \, dxdy \tag{13}$$

It's worth to mention that equation of motions become non-homogenous due to presence of follower force according to Eq. (12).

7 HAMILTON'S PRINCIPLE

Hamilton's principle is used to derive the motion equations. The principle can be stated in an analytical form where the first variation form of motion equations must be zero, as follows [20]:

$$\int_{t_1}^{t_2}\left[\delta U_{Sandwich} - (\delta K_{Sandwich} + \delta\Sigma)\right]dt = 0 \tag{14}$$

where $\delta U_{Sandwich}, \delta K_{Sandwich}$ and $\delta\Sigma$ are variation of strain energy, variation of Kinetic energy and variation of external work. Substituting Eqs. (10,11,12) into Eq. (13) for TSDT and using dimensionless parameters which introduced

in Eq. (14):

$$\begin{aligned}
&(\zeta,\eta) = \left(\frac{x}{a},\frac{y}{b}\right), \quad (U,V,W) = \left(\frac{u_0}{a},\frac{v_0}{b},\frac{w_0}{h}\right), \quad For \begin{cases} Core: h_c \\ Face\,sheet: h_m \end{cases} \\
&\gamma = \frac{a}{b}, Q_{ij} = \frac{\bar{Q}_{ij}}{E_m}, C_{ij} = \frac{\bar{C}_{ij}}{E_m}, \in = \frac{E_c}{E_m}, \delta = \frac{h_c}{h_m}, \quad (\alpha_m,\beta_m) = \left(\frac{h_m}{a},\frac{h_m}{b}\right), \ (\alpha_c,\beta_c) = \left(\frac{h_c}{a},\frac{h_c}{b}\right), \\
&G_{ij} = \frac{e_{ij}\,C(t)K_c}{\sqrt{E_m\rho_m}}, \quad \tau = \frac{t}{a}\sqrt{\frac{E_m}{\rho_m}}, \quad Ibi = \frac{Ii}{h_m^{i+1}} \ (i = 2,4,6), q_b = \frac{q}{E_m}
\end{aligned} \tag{15}$$

The equations of motion are obtained by setting the coefficient $\delta U, \delta V, \delta W, \delta\theta_1, \delta\theta_2$ equal to zero as follows:

$$\delta U = \delta U_{core} + \delta U_{Sheet} = (-1/2C_{44}\beta\gamma\frac{d^2U}{d\eta^2} - C_{11}\alpha\frac{d^2U}{d\zeta^2} - 1/2C_{44}\alpha\frac{d^2V}{d\eta d\zeta} - 1/2C_{21}\alpha\frac{d^2V}{d\eta d\zeta}$$
$$-1/2C_{12}\alpha\frac{d^2V}{d\eta d\zeta} + \alpha\epsilon\frac{d^2U}{d\tau^2})_{Core} + (-2Q_{11}\alpha_m\frac{d^2U}{d\zeta^2} - Q_{44}\gamma\beta_m\frac{d^2U}{d\eta^2} + G_{31}\alpha_m{}^2\frac{d^2W}{d\tau d\zeta} \quad (16a)$$
$$-Q_{44}\alpha_m\frac{d^2V}{d\eta d\zeta} - Q_{12}\alpha_m\frac{d^2V}{d\eta d\zeta} - Q_{21}\alpha_m\frac{d^2V}{d\eta d\zeta} + 2\alpha_m\frac{d^2U}{d\tau^2})_{Sheet},$$

$$\delta V = \delta V_{Core} + \delta V_{Sheet} = (-1/2\gamma C_{44}\alpha\frac{d^2V}{d\zeta^2} - C_{22}\beta\frac{d^2V}{d\eta^2} - 1/2C_{44}\beta\frac{d^2U}{d\eta d\zeta} - 1/2C_{21}\beta\frac{d^2U}{d\eta d\zeta}$$
$$-1/2C_{12}\beta\frac{d^2U}{d\eta d\zeta} + \frac{\alpha}{\gamma}\epsilon\frac{d^2V}{d\tau^2})_{Core} + (-2Q_{22}\beta_m\frac{d^2V}{d\eta^2} - \frac{Q_{44}\alpha_m}{\gamma}\frac{d^2V}{d\zeta^2} + G_{32}\alpha_m\beta_m\frac{d^2W}{d\tau d\eta} \quad (16b)$$
$$-Q_{44}\beta_m\frac{d^2U}{d\eta d\zeta} - Q_{12}\beta_m\frac{d^2U}{d\eta d\zeta} - Q_{21}\beta_m\frac{d^2U}{d\eta d\zeta} + 2\frac{\alpha_m}{\gamma}\frac{d^2V}{d\tau^2})_{Sheet},$$

$$\delta W = \delta W_{Core} + \delta W_{Sheet} = (-\frac{4}{15}C_{55}\alpha^2\frac{d^2W}{d\zeta^2} - \frac{4}{15}C_{66}\beta^2\frac{d^2W}{d\eta^2} - \frac{2}{315}C_{12}\alpha^2\beta\frac{d^3\theta_2}{d\eta\zeta^2} - \frac{2}{315}C_{21}\alpha^2\beta\frac{d^3\theta_2}{d\eta\zeta^2}$$
$$-\frac{4}{315}C_{44}\beta^2\alpha\frac{d^3\theta_1}{d\eta^2 d\zeta} - \frac{2}{315}C_{21}\beta^2\alpha\frac{d^3\theta_1}{d\eta^2 d\zeta} - \frac{4}{315}C_{22}\beta^3\frac{d^3\theta_2}{d\eta^3} - \frac{4}{315}C_{11}\alpha^3\frac{d^3\theta_1}{d\zeta^3} - \frac{4}{315}C_{44}\alpha^2\beta\frac{d^3\theta_2}{d\eta\zeta^2}$$
$$-\frac{4}{15}C_{55}\alpha\frac{d\theta_1}{d\zeta} - \frac{2}{315}C_{12}\beta^2\alpha\frac{d^3\theta_1}{d\eta^2 d\zeta} - 1/2C_{66}\beta\frac{d\theta_2}{d\eta} + \frac{7}{30}C_{66}\alpha\frac{d\theta_2}{d\eta} + \frac{1}{252}C_{22}\beta^4\frac{d^4W}{d\eta^4} + \frac{1}{126}C_{44}\alpha^2\beta^2\frac{d^4W}{d\eta^2 d\zeta^2}$$
$$+\frac{1}{252}C_{11}\alpha^4\frac{d^4W}{d\zeta^4} + \frac{1}{252}C_{12}\alpha^2\beta^2\frac{d^4W}{d\eta^2 d\zeta^2} + \frac{1}{252}C_{21}\alpha^2\beta^2\frac{d^4W}{d\eta^2 d\zeta^2} + \frac{4}{315}\alpha^3\epsilon\frac{d^3\theta_1}{d\tau^2 d\zeta} - \frac{1}{252}\alpha^4\epsilon\frac{d^4W}{d\tau^2 d\zeta^2}$$
$$+\frac{4}{315}\alpha^2\beta\epsilon\frac{d^3\theta_2}{d\tau^2 d\eta} - \frac{1}{252}\alpha^2\beta^2\epsilon\frac{d^4W}{d\tau^2 d\eta^2} + \alpha^2\epsilon\frac{d^2W}{d\tau^2})_{Core} + (\frac{32}{9}Q_{22}Ib6\beta_m{}^4\frac{d^4W}{d\eta^4} + \frac{32}{9}Q_{11}Ib6\alpha_m{}^4\frac{d^4W}{d\zeta^4}$$
$$+8Q_{55}Ib2\alpha_m{}^2\frac{d^2W}{d\zeta^2} - 16Q_{66}Ib4\beta_m{}^2\frac{d^2W}{d\eta^2} + 8Q_{66}Ib2\beta_m{}^2\frac{d^2W}{d\eta^2} - 16Q_{55}Ib4\alpha_m{}^2\frac{d^2W}{d\zeta^2} - \frac{32}{9}Ib6\alpha_m{}^2\beta_m{}^2\frac{d^4W}{d\tau^2 d\eta^2}$$
$$-8/3Q_{11}Ib4\alpha_m{}^3\frac{d^3\theta_1}{d\zeta^3} + \frac{32}{9}Q_{11}Ib6\alpha_m{}^3\frac{d^3\theta_1}{d\zeta^3} - 16Q_{55}Ib4\alpha_m\frac{d\theta_1}{d\zeta} + 8Q_{55}Ib2\alpha_m\frac{d\theta_1}{d\zeta} - 8/3Q_{22}Ib4\beta_m{}^3\frac{d^3\theta_2}{d\eta^3} \quad (16c)$$
$$+\frac{32}{9}Q_{22}Ib6\beta_m{}^3\frac{d^3\theta_2}{d\eta^3} + 8/3Ib4\alpha_m{}^2\beta_m\frac{d^3\theta_2}{d\tau^2 d\eta} - \frac{32}{9}Ib6\alpha_m{}^2\beta_m\frac{d^3\theta_2}{d\tau^2 d\eta} - 16Q_{66}Ib4\beta_m\frac{d\theta_2}{d\eta} + 8Q_{66}Ib2\beta_m\frac{d\theta_2}{d\eta}$$
$$+2\alpha_m{}^2\frac{d^2W}{d\tau^2} + G_{31}\alpha_m\frac{d^2U}{d\tau d\zeta} + G_{32}\alpha_m\frac{d^2V}{d\tau d\eta} - Q_{55}\alpha_m{}^2\frac{d^2W}{d\zeta^2} + 8/3Ib4\alpha_m{}^3\frac{d^3\theta_1}{d\tau^2 d\zeta} - \frac{32}{9}Ib6\alpha_m{}^4\frac{d^4W}{d\tau^2 d\zeta^2}$$
$$-Q_{66}\beta_m{}^2\frac{d^2W}{d\eta^2} - \frac{32}{9}Ib6\alpha_m{}^3\frac{d^3\theta_1}{d\tau^2 d\zeta} - Q_{66}\beta_m\frac{d\theta_2}{d\eta} - Q_{55}\alpha_m\frac{d\theta_1}{d\zeta} + \frac{16}{9}Q_{21}Ib6\beta_m{}^2\alpha_m\frac{d^3\theta_1}{d\eta^2 d\zeta}$$
$$-4/3Q_{12}Ib4\beta_m{}^2\alpha_m\frac{d^3\theta_1}{d\eta^2 d\zeta} + \frac{32}{9}Q_{44}Ib6\beta_m{}^2\alpha_m\frac{d^3\theta_1}{d\eta^2 d\zeta} - 4/3Q_{21}Ib4\beta_m{}^2\alpha_m\frac{d^3\theta_1}{d\eta^2 d\zeta} + \frac{16}{9}Q_{12}Ib6\beta_m{}^2\alpha_m\frac{d^3\theta_1}{d\eta^2 d\zeta}$$
$$-8/3Q_{44}Ib4\beta_m{}^2\alpha_m\frac{d^3\theta_1}{d\eta^2 d\zeta} + \frac{32}{9}Q_{44}Ib6\alpha_m{}^2\beta_m\frac{d^3\theta_2}{d\eta d\zeta^2} - 4/3Q_{21}Ib4\alpha_m{}^2\beta_m\frac{d^3\theta_2}{d\eta d\zeta^2} - 4/3Q_{12}Ib4\alpha_m{}^2\beta_m\frac{d^3\theta_2}{d\eta d\zeta^2}$$
$$-8/3Q_{44}Ib4\alpha_m{}^2\beta_m\frac{d^3\theta_2}{d\eta d\zeta^2} + \frac{16}{9}Q_{21}Ib6\alpha_m{}^2\beta_m\frac{d^3\theta_2}{d\eta d\zeta^2} + \frac{16}{9}Q_{12}Ib6\alpha_m{}^2\beta_m\frac{d^3\theta_2}{d\eta d\zeta^2} + \frac{64}{9}Q_{44}Ib6\alpha_m{}^2\beta_m{}^2\frac{d^4W}{d\eta^2 d\zeta^2}$$
$$+\frac{32}{9}Q_{12}Ib6\alpha_m{}^2\beta_m{}^2\frac{d^4W}{d\eta^2 d\zeta^2} + \frac{32}{9}Q_{21}Ib6\alpha_m{}^2\beta_m{}^2\frac{d^4W}{d\eta^2 d\zeta^2}w_0 + q_b\alpha_m(1-\zeta)\frac{d^2W}{d\zeta^2})_{Sheet},$$

$$\delta\theta_1=\delta\theta_{1Core}+\delta\theta_{1Sheet}=(\frac{23}{30}C_{55}\delta\theta_1+\frac{2}{315}C_{12}\delta\beta^2\alpha\frac{d^3W}{d\eta^2d\zeta}+\frac{4}{315}C_{44}\delta\beta^2\alpha\frac{d^3W}{d\eta^2d\zeta}+\frac{2}{315}C_{21}\delta\beta^2\alpha\frac{d^3W}{d\eta^2d\zeta}$$
$$-\frac{17}{630}C_{12}\delta\beta\alpha\frac{d^2\theta_2}{d\eta\zeta}-\frac{17}{630}C_{44}\delta\beta\alpha\frac{d^2\theta_2}{d\eta\zeta}+\frac{4}{315}C_{11}\delta\alpha^3\frac{d^3W}{d\zeta^3}-\frac{17}{630}C_{21}\delta\beta\alpha\frac{d^2\theta_2}{d\eta\zeta}+\frac{4}{15}C_{55}\delta\alpha\frac{dW}{d\zeta}$$
$$-\frac{17}{630}C_{44}\delta\beta^2\frac{d^2\theta_1}{d\eta^2}-\frac{17}{315}C_{11}\delta\alpha^2\frac{d^2\theta_1}{d\zeta^2}+\frac{17}{315}\delta\alpha^2\epsilon\frac{d^2\theta_1}{d\tau^2}-\frac{4}{315}\delta\alpha^3\epsilon\frac{d^3W}{d\tau^2d\zeta})_{Core}+(Q_{55}\theta_1-\frac{32}{9}Q_{11}Ib6\alpha_m^3\frac{d^3W}{d\zeta^3}$$
$$-8Q_{55}Ib2\alpha_m\frac{dW}{d\zeta}+16Q_{55}Ib4\alpha_m\frac{dW}{d\zeta}+8/3Q_{44}Ib4\beta_m{}^2\frac{d^2\theta_1}{d\eta^2}-\frac{16}{9}Q_{44}Ib6\beta_m{}^2\frac{d^2\theta_1}{d\eta^2}+16/3Q_{11}Ib4\alpha_m{}^2\frac{d^2\theta_1}{d\zeta^2}$$
$$-\frac{32}{9}Q_{11}Ib6\alpha_m^2\frac{d^2\theta_1}{d\zeta^2}-Q_{44}Ib2\beta_m^2\frac{d^2\theta_1}{d\eta^2}-2Q_{11}Ib2\beta_m^2\frac{d^2\theta_1}{d\zeta^2}+8/3Q_{11}Ib4\alpha_m^3\frac{d^3W}{d\zeta^3}+4/3Q_{21}Ib4\beta_m^2\alpha_m\frac{d^3W}{d\eta^2d\zeta} \quad (16d)$$
$$+4/3Q_{12}Ib4\beta_m^2\alpha_m\frac{d^3W}{d\eta^2d\zeta}-\frac{32}{9}Q_{44}Ib6\beta_m^2\alpha_m\frac{d^3W}{d\eta^2d\zeta}-\frac{16}{9}Q_{21}Ib6\beta_m^2\alpha_m\frac{d^3W}{d\eta^2d\zeta}-\frac{16}{9}Q_{12}Ib6\beta_m^2\alpha_m\frac{d^3W}{d\eta^2d\zeta}$$
$$+8/3Q_{44}Ib4\beta_m{}^2\alpha_m\frac{d^3W}{d\eta^2d\zeta}-Q_{21}Ib2\beta_m\alpha_m\frac{d^2\theta_2}{d\eta\mathrm{d}\zeta}+8/3Q_{21}Ib4\beta_m\alpha_m\frac{d^2\theta_2}{d\eta d\zeta}-\frac{16}{9}Q_{12}Ib6\beta_m\alpha_m\frac{d^2\theta_2}{d\eta\zeta}$$
$$-\frac{16}{9}Q_{44}Ib6\beta_m\alpha_m\frac{d^2\theta_2}{d\eta\mathrm{d}\zeta}-\frac{16}{9}Q_{21}Ib6\beta_m\alpha_m\frac{d^2\theta_2}{d\eta\mathrm{d}\zeta}+8/3Q_{44}Ib4\beta_m\alpha_m\frac{d^2\theta_2}{d\eta\mathrm{d}\zeta}+8/3Q_{12}Ib4\beta_m\alpha_m\frac{d^2\theta_2}{d\eta\mathrm{d}\zeta}$$
$$-Q_{12}Ib2\beta_m\alpha_m\frac{d^2\theta_2}{d\eta\mathrm{d}\zeta}-Q_{44}Ib2\beta_m\alpha_m\frac{d^2\theta_2}{d\eta\mathrm{d}\zeta}+\frac{32}{9}Ib6\alpha_m{}^2\frac{d^2\theta_1}{d\tau^2}+2Ib2\alpha_m{}^2\frac{d^2\theta_1}{d\tau^2}+\frac{32}{9}Ib6\alpha_m{}^3\frac{d^3W}{d\tau^2d\zeta}$$
$$-8Q_{55}Ib2\theta_1-16/3Ib4\alpha_m{}^2\frac{d^2\theta_1}{d\tau^2}+16Q_{55}Ib4\theta_1-8/3Ib4\alpha_m{}^3\frac{d^3W}{d\tau^2d\zeta}+Q_{55}\alpha_m\frac{dW}{d\zeta})_{Sheet},$$

$$\delta\theta_2=\delta\theta_{2Core}+\delta\theta_{2Sheet}=(\frac{4}{15}C_{66}\delta\theta_2+\frac{2}{315}C_{12}\delta\alpha^2\beta\frac{d^3W}{d\eta\zeta^2}+\frac{2}{315}C_{21}\delta\alpha^2\beta\frac{d^3W}{d\eta\zeta^2}-\frac{17}{630}C_{12}\delta\alpha\beta\frac{d^2\theta_1}{d\eta\zeta}$$
$$+\frac{4}{315}C_{22}\delta\beta^3\frac{d^3W}{d\eta^3}-\frac{17}{630}C_{44}\delta\alpha\beta\frac{d^2\theta_1}{d\eta\zeta}+\frac{4}{315}C_{44}\delta\alpha^2\beta\frac{d^3W}{d\eta\zeta^2}-\frac{17}{630}C_{21}\delta\alpha\beta\frac{d^2\theta_1}{d\eta\zeta}+\frac{4}{15}C_{66}\delta\beta\frac{dW}{d\eta}$$
$$-\frac{17}{630}C_{44}\delta\alpha^2\frac{d^2\theta_2}{d\zeta^2}-\frac{17}{315}C_{22}\delta\beta^2\frac{d^2\theta_2}{d\eta^2}+\frac{17}{315}\delta\alpha^2\epsilon\frac{d^2\theta_2}{d\tau^2}-\frac{4}{315}\delta\alpha^3\epsilon\frac{d^3W}{d\tau^2d\zeta})_{Core}+Q_{66}\theta_2+Q_{66}\beta_m\frac{dW}{d\eta}$$
$$+16Q_{66}Ib4\theta_2+2Ib2\alpha_m^2\frac{d^2\theta_2}{d\tau^2}+4/3Q_{12}Ib4\beta_m\alpha_m^2\frac{d^3W}{d\eta\mathrm{d}\zeta^2}-\frac{32}{9}Q_{44}Ib6\beta_m\alpha_m^2\frac{d^3W}{d\eta\mathrm{d}\zeta^2}+4/3Q_{21}Ib4\beta_m\alpha_m^2\frac{d^3W}{d\eta\mathrm{d}\zeta^2}$$
$$-\frac{16}{9}Q_{12}Ib6\beta_m\alpha_m{}^2\frac{d^3W}{d\eta\mathrm{d}\zeta^2}-\frac{16}{9}Q_{21}Ib6\beta_m\alpha_m{}^2\frac{d^3W}{d\eta\mathrm{d}\zeta^2}+8/3Q_{44}Ib4\beta_m\alpha_m{}^2\frac{d^3W}{d\eta\mathrm{d}\zeta^2}-\frac{16}{9}Q_{44}Ib6\beta_m\alpha_m\frac{d^2\theta_1}{d\eta\mathrm{d}\zeta} \quad (16e)$$
$$-\frac{16}{9}Q_{21}Ib6\beta_m\alpha_m\frac{d^2\theta_1}{d\eta\mathrm{d}\zeta}-Q_{21}Ib2\beta_m\alpha_m\frac{d^2\theta_1}{d\eta\mathrm{d}\zeta}-Q_{12}Ib2\beta_m\alpha_m\frac{d^2\theta_1}{d\eta\mathrm{d}\zeta}+8/3Q_{12}I4b\beta_m\alpha_m\frac{d^2\theta_1}{d\eta\mathrm{d}\zeta}$$
$$-Q_{44}Ib2\beta_m\alpha_m\frac{d^2\theta_1}{d\eta\mathrm{d}\zeta}+8/3Q_{44}Ib4\beta_m\alpha_m\frac{d^2\theta_1}{d\eta\mathrm{d}\zeta}+8/3Q_{21}Ib4\beta_m\alpha_m\frac{d^2\theta_1}{d\eta\mathrm{d}\zeta}-\frac{16}{9}Q_{12}Ib6\beta_m\alpha_m\frac{d^2\theta_1}{d\eta\mathrm{d}\zeta}$$
$$-8Q_{66}Ib2\beta_m\frac{dW}{d\eta}+16Q_{66}Ib4\beta_m\frac{dW}{d\eta}+8/3Q_{22}Ib4\beta_m{}^3\frac{d^3W}{d\eta^3}-\frac{32}{9}Q_{22}Ib6\beta_m{}^3\frac{d^3W}{d\eta^3}-8/3Ib4\beta_m\alpha_m{}^2\frac{d^3W}{d\tau^2d\eta}$$
$$+\frac{32}{9}Ib6\beta_m\alpha_m^2\frac{d^3W}{d\tau^2d\eta}-\frac{32}{9}Q_{22}Ib6\beta_m^2\frac{d^2\theta_2}{d\eta^2}-\frac{16}{9}Q_{44}Ib6\alpha_m^2\frac{d^2\theta_2}{d\zeta^2}+8/3Q_{44}Ib4\alpha_m^2\frac{d^2\theta_2}{d\zeta^2}+16/3Q_{22}Ib4\beta_m^2\frac{d^2\theta_2}{d\eta^2}$$
$$-2Ib2\beta_m{}^2Q_{22}\frac{d^2\theta_2}{d\eta^2}-Q_{44}Ib2\alpha_m{}^2\frac{d^2\theta_2}{d\zeta^2}+\frac{32}{9}Ib6\alpha_m{}^2\frac{d^2\theta_2}{d\tau^2}-8Q_{66}Ib2\theta_2-16/3Ib4\alpha_m{}^2\frac{d^2\theta_2}{d\tau^2})_{Sheet}$$

where

$$Ii=\int_{h_c/2}^{(h_c/2+h_m)}z^i\,dz+\int_{-(h_c/2+h_m)}^{-h_c/2}z^i\,dz,\qquad(i=2,4,6)$$

8 SOLUTION PROCEDURE USING DQM

At first Eq. (16) is used for separation of variables in space and time:

$$\begin{aligned} U(\zeta,\eta,\tau) &= U(\zeta,\eta)\ e^{\omega\tau}, \\ V(\zeta,\eta,\tau) &= V(\zeta,\eta)\ e^{\omega\tau}, \\ W(\zeta,\eta,\tau) &= W(\zeta,\eta)\ e^{\omega\tau}, \\ \theta_1(\zeta,\eta,\tau) &= \theta_1(\zeta,\eta)\ e^{\omega\tau}, \\ \theta_2(\zeta,\eta,\tau) &= \theta_2(\zeta,\eta)\ e^{\omega\tau} \end{aligned} \tag{17}$$

where $\omega = \Omega a\sqrt{\rho_m}/\sqrt{E_m}$ is the dimensionless frequency (Ω is the dimensional frequency). In DQM, the differential equations change into the first algebraic equations where the partial derivatives of a function (F) are approximated by a specific variable, at discontinuous points by a set of weighting series. It's supposed that F be a function representing U, V, W, θ_1 and θ_2 with respect to variables ξ and η $(0 \prec \xi \prec 1,\ 0 \prec \eta \prec 1)$ when $N_\xi \times N_\eta$ be the grid points along these variables with following derivative [21]:

$$\begin{aligned} \frac{d^n F(\xi_i,\eta_j)}{d\xi^n} &= \sum_{k=1}^{N_\xi} A_{ik}^{(n)} F(\xi_k,\eta_j) \qquad n = 1,...,N_\xi - 1, \\ \frac{d^m F(\xi_i,\eta_j)}{d\eta^m} &= \sum_{l=1}^{N_\eta} B_{jl}^{(m)} F(\xi_i,\eta_l) \qquad m = 1,...,N_\eta - 1, \\ \frac{d^{n+m} F(\xi_i,\eta_j)}{d\xi^n d\eta^m} &= \sum_{k=1}^{N_\xi}\sum_{l=1}^{N_\eta} A_{ik}^{(n)} B_{jl}^{(m)} F(\xi_k,\eta_l) \end{aligned} \tag{18}$$

where $A_{ik}^{(n)}$ and $B_{jl}^{(m)}$ are the weighting coefficients using Chebyshev polynomials for the positions of the grid points whose recursive formulae can be found in [21]. Applying DQM and using Eq. (17) into governing Eqs. (16), the standard form of vibrational motion equation set $(M\ddot{X} + C\dot{X} + KX = 0 \rightarrow M\omega^2 + C\omega + K = 0)$ are obtained and by considering simply supported boundary conditions an eigenvalue problem is derived in which the Eigen-values of state-space matrix $\left([\text{state}-\text{space}] = \begin{bmatrix} [0] & [\text{I}] \\ -[\text{M K}] & -[\text{M C}] \end{bmatrix}\right)$ are the dimensionless frequency. Eigenvalues are obtained as $\omega_{1,2} = -\zeta\omega_n \pm i\,\omega_n\sqrt{1-\zeta^2}$ where $\omega_n = \sqrt{K/M}$ is the natural frequency and $\zeta = C/(2\sqrt{KM})$. It is clear that the imaginary part of Eigen-values is introduced as dimensionless frequency $(\omega_n\sqrt{1-\zeta^2})$. It is worth to mention that M is the mass matrix, C is the damping matrix and K is the stiffness, $[\text{I}]$ and $[0]$ are the unitary and zero matrixes.

9 NUMERICAL RESULTS AND DISCUSSION

In this work, free vibration of sandwich plate were analyzed when the plate subjected to follower forces. Sandwich plate were contained an elastic composite core that reinforced by CNT fibers. The fibers were uniformly distributed and their material properties obtained by rule of Mixture. Two smart face sheets were surrounded the CNTRC core where the three layers vibrated as an integrated sandwich. A feedback system was used to control the vibration of sandwich plate in presence of magnetic field. Then the vibration response of sandwich plate was investigated by stimulus factors such as velocity feedback gain, core-to-face sheet thickness ratio, volume fraction of fibers, temperature, follower forces. The face sheet has been made of Terfenol-D and its properties are listed at Table 4.

Table 4
Material properties of face sheet (Terfnol_D) and matrix (*PmPV*).[4,8]

Properties	E	υ	ρ	$e31=e32$
Terfenol-D	$30e9\,Pa$	0.25	$9.25\times10^3\,kg/m^3$	$442.55\,N/(m.A)$
PmPV	$(3.51-0.0047T)\,GPa$	0.34	$1190\,kg/m^3$	-

At first, to ensure the correct results, linear frequency $\omega=\Omega a^2\sqrt{\frac{\rho.h}{D}}$, $D=\frac{EI}{(1-\upsilon^2)}$ for an isotropic square plate has been compared in Table 5 for three modes. A good agreement among the results of present work and other published papers (Refs. [3,22]) show the correct solution is used.

Table 5
Comparison of linear frequency for an isotropic square plate $(\gamma=1,\ \beta=1/300,\ \upsilon=0.3)$.

	ω11	ω12	ω13
Leissa [22]	19.7392	49.3480	98.6960
Wang and Shen [3]	19.7362	49.3431	98.6765
Present work	19.4250	49.3392	98.0423

Obtained frequencies from equations of motion are complex values that Figs. 2 to 5 indicate separately the imaginary and real parts of frequency. As can be seen, when the system is stable, $\mathrm{Im}(\omega)$ decreases with increasing q_b, while the $\mathrm{Re}(\omega)$ is zero. The critical follower force is the point in which the frequency becomes zero, after it, the stability of system loses. In fact, the system at critical point becomes susceptible to buckling.

Fig. 2(a) and 2(b) displays the effect of core-to-face sheet thickness ratio on dimensional frequency when the composite-faced sheet plate reinforced by CNT with $h=0.34\,nm$. In Fig. 2(a) the critical value for follower force is $q_b\approx0.062$ for $\delta=22$ in the first mode and this value increases by increasing δ that named core-to-face sheet thickness ratio. The result shows that the sandwich plate with magneto-strictive face sheets has a higher dimensionless frequency than the same plate with CNTRC core.

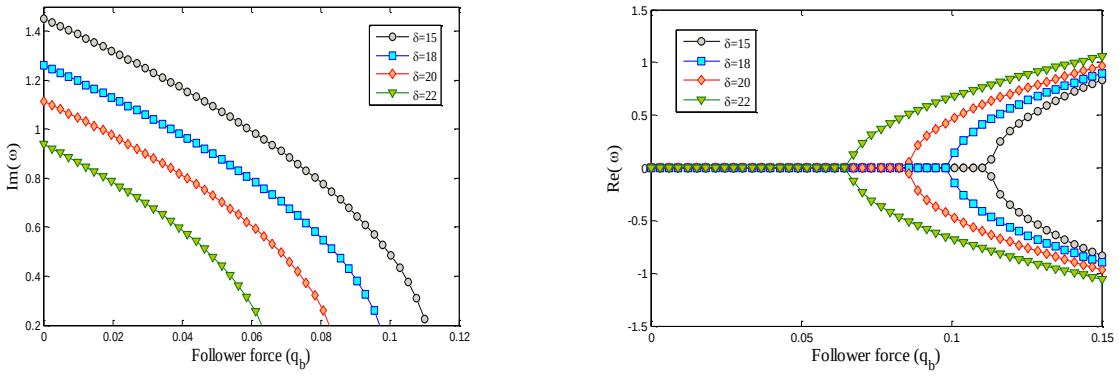

(a) (b)

Fig.2
a) Variation of Imaginary part of dimensionless frequency versus follower force for different δ. b) Variation of real part of dimensionless frequency versus follower force for different δ.

The effect of velocity feedback gain $K_cC(t)$ on imaginer and real parts of dimensionless frequency illustrates in Fig. 3(a) and 3(b). Velocity feedback gain as a control parameter can be used to reduce the frequency of sandwich plate. In the other hand, magnetic field significantly influences on vibrational behavior of system where in presence of follower force the changes in velocity feedback gain cause to considerable change in frequency. Increasing the velocity feedback gain leads to decrease the dimensionless frequency significantly. Fig. 3(a) and 3(b) has been

plotted for four values of velocity feedback gain which three of them are close together. It worth to mention that $K_c C(t) = 0$ means uncontrolled system.

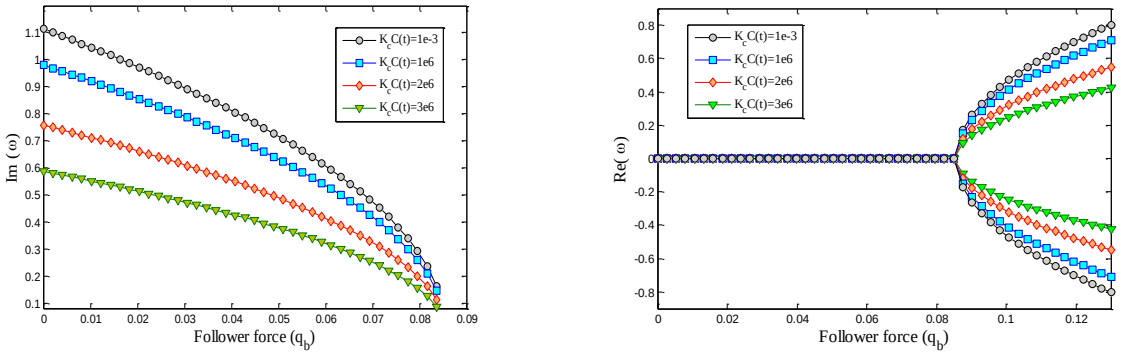

(a) (b)

Fig.3

a) Variation of Imaginary part of dimensionless frequency versus follower force for different $K_c C(t)$. b) Variation of real part of dimensionless frequency versus follower force for different $K_c C(t)$.

Since the material properties of CNT fibers have been reported for different temperature, Fig. 4(a) and 4(b) shows the vibrational response of sandwich plate in these temperatures. It's clear from the imaginary and real parts of figure that increasing the temperature leads to decrease the dimensionless frequency because the elastic properties of CNT such as Young and shear modulus change so that the structure becomes softer.

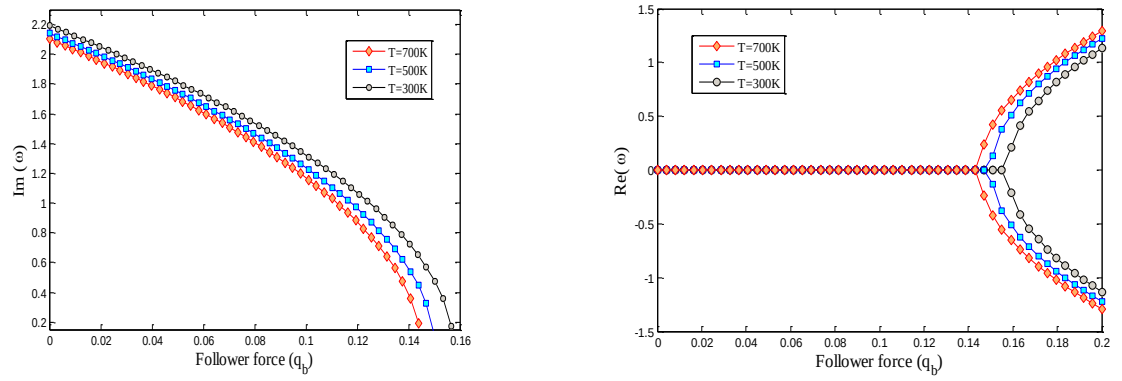

(a) (b)

Fig.4

a) Variation of Imaginary part of dimensionless frequency versus follower force for different temperatures. b) Variation of real part of dimensionless frequency versus follower force for different temperatures.

Figs. 5(a) and 5(b) show the effect of volume fraction of CNT as a fibers of composite core on dimensionless frequency. There are three case for volume fraction of CNTs in which the material properties has been compared with MD results according to the rule of Mixture. CNT efficiency parameter and other elastic properties have been reported in Tables 1 to 3. Imaginary and real parts of frequency in Figs. 5(a) and 5(b) clearly show the effect of fibers on strength of the core where increasing volume fraction from $V_{CNT} = 0.11 to\ 0.17$ leads to increase the dimensionless frequency significantly.

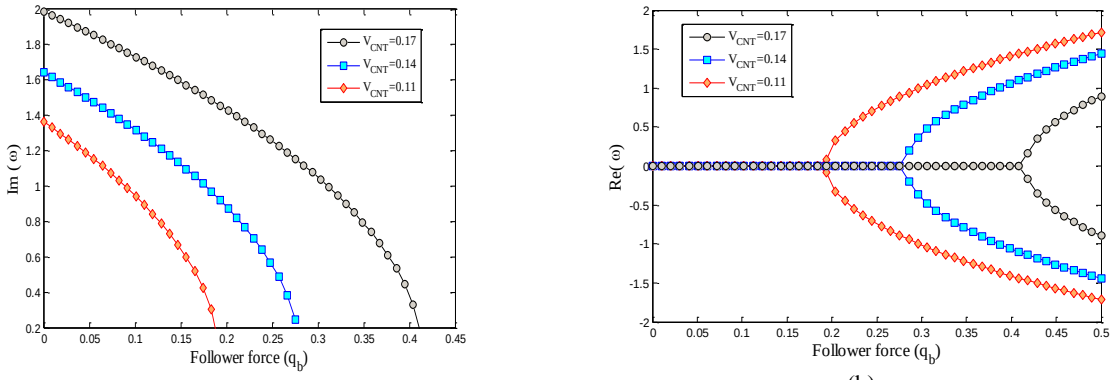

(a) (b)

Fig.5

a) Variation of Imaginary part of dimensionless frequency versus follower force for different V_{CNT} . b) Variation of real part of dimensionless frequency versus follower force for different V_{CNT} .

10 CONCLUSIONS

Vibration response of sandwich plate with nano-composite core and magneto-strictive face sheets is a novel topic that has been studied in this research for the first time. To consider the magnetization effect of face sheet, a control feedback system was used and velocity feedback gain as controlling parameter introduced. Sandwich plate undergoes the follower forces in the opposite direction of x axis. Reddy's plate as a third order shear deformation plat theory was used to derive the equations of motion. Set of equations were solved by two-dimensional DQM and following results were concluded:

- Follower force has damping effect on vibration of sandwich plate so that with increasing the follower force, the sandwich plate behaves divergent instability in the first-order mode.
- Both face sheets can be utilized to vibration suppression of sandwich plate using control feedback system where velocity feedback gain as a control parameter reduces the frequency of sandwich plate. Also the effect of velocity feedback gain continues so far the frequency tends to constant value for all of parameters but it's possible for very precise controller.
- Sandwich plate with magneto-strictive face sheets has a higher dimensionless frequency than the same plate with CNTRC core. This refers to the material properties of face sheets and core.
- Dimensionless frequency of composite core with higher volume fraction of fibers is larger.

ACKNOWLEDGEMENTS

The author would like to thank the reviewers for their comments and suggestions to improve the clarity of this article.

REFERENCES

[1] Reddy J.N., 2004, *Mechanics of Laminated Composite Plates and Shells: Theory and Analysis*, CRC Press, Boca Raton.

[2] Panda S., Ray M.C., 2009, Active control of geometrically nonlinear vibrations of functionally graded laminated composite plates using piezoelectric fiber reinforced composites, *Journal of Sound and Vibration* **325**(1-2): 186-205.

[3] Wang Z.X., Shen H.S., 2012, Nonlinear vibration and bending of sandwich plates with nanotube-reinforced composite face sheets, *Composites Part B-Engineering* **43**(2): 411-421.

[4] Lei Z.X., Liew K.M., Yu J.L., 2013, Free vibration analysis of functionally graded carbon nanotube-reinforced composite plates using the element-free kp-Ritz method in thermal environment, *Composite Structures* **106**: 128-138.

[5] Natarajan S., Haboussi M., Manickam G., 2014, Application of higher-order structural theory to bending and free vibration analysis of sandwich plates with CNT reinforced composite face sheets, *Composite Structures* **113**: 197-207.

[6] Malekzadeh K., Khalili S.M.R., Abbaspour P., 2010, Vibration of non-ideal simply supported laminated plate on an elastic foundation subjected to in-plane stresses, *Composite Structures* **92**: 1478-1484.
[7] Lee S.J., Reddy J.N., Rostam-Abadi F., 2004, Transient analysis of laminate embedded smart-material layers, *Finite Elements in Analysis and Design* **40**(5-6): 463-483.
[8] Hong C.C., 2010, Transient responses of magneto-strictive plates by using the GDQ method, *European Journal of Mechanics A-Solids* **29**(6): 1015-1021.
[9] Kim J.H., Kim H.S., 2000, A study on the dynamic stability of plates under a follower force, *Computers and Structures* **74**: 351-363.
[10] Jayaraman G., Struthers A., 2005, Divergence and flutter instability of elastic specially orthotropic plates subject to follower forces, *Journal of Sound and Vibration* **281**: 357-373.
[11] Guo X., Wang Z., Wang Y., 2011, Dynamic stability of thermoelastic coupling moving plate subjected to follower force, *Applied Acoustics* **72**: 100-107.
[12] Pourasghar A., Kamarian S., 2013, Dynamic stability analysis of functionally graded nanocomposite non-uniform column reinforced by carbon nanotube, *Journal of Vibration and Control* **21**: 2499-2508.
[13] Shen H.S., 2009, Nonlinear bending of functionally graded carbon nanotube reinforced composite plates in thermal environments, *Composite Structures* **91**: 9-19.
[14] Han Y., Elliott J., 2007, Molecular dynamics simulations of the elastic properties of polymer/carbon nanotube composites, *Computational Materials Science* **39**(2): 315-323.
[15] Hong C.C., 2009, Transient responses of magneto-strictive plates without shear effects, *International Journal of Engineering Science* **47**(3): 355-362.
[16] Krishna M., Anjanappa M., Wu Y.F., 1997, The use of magneto-strictive particle actuators for vibration attenuation of flexible beams, *Journal of Sound and Vibration* **206**(2): 133-149.
[17] Daneshmehr A., Rajabpoor A., Pourdavood M., 2014, Stability of size dependent functionally graded nano-plate based on nonlocal elasticity and higher order plate theories and different boundary conditions, *International Journal of Engineering Science* **82**: 84-100.
[18] Wang C.M., Reddy J.N., Lee K.H. 2000, *Shear Deformable Beams and Plates*, Elsevier Science Ltd, UK.
[19] Reddy J.N., 2000, *Energy Principles and Variational Methods in Applied Mechanics*,John Wiley and Sons Publishers, Texas.
[20] Ghorbanpour Arani A., Vossough H., Kolahchi R., Mosallaie Barzoki A.A., 2012, Electro-thermo nonlocal nonlinear vibration in an embedded polymeric piezoelectric micro plate reinforced by DWBNNTs using DQM, *Journal of Mechanical Science and Technology* **26**(10): 3047-3057.
[21] Shu C., 2000, *Differential Quadrature and its Application in Engineering*, Singapore, Springer publishers.
[22] Leissa A.W., 1973, The free vibration of rectangular plates, *Journal of Sound and Vibration* **31**(3): 257-293.